ORIGINAL ARTICLE

Translational Pharmacometric Evaluation of Typical Antibiotic Broad-Spectrum Combination Therapies Against *Staphylococcus Aureus* Exploiting *In Vitro* Information

SG Wicha[1], W Huisinga[2] and C Kloft[1]*

Broad-spectrum antibiotic combination therapy is frequently applied due to increasing resistance development of infective pathogens. The objective of the present study was to evaluate two common empiric broad-spectrum combination therapies consisting of either linezolid (LZD) or vancomycin (VAN) combined with meropenem (MER) against *Staphylococcus aureus* (*S. aureus*) as the most frequent causative pathogen of severe infections. A semimechanistic pharmacokinetic-pharmacodynamic (PK-PD) model mimicking a simplified bacterial life-cycle of *S. aureus* was developed upon time-kill curve data to describe the effects of LZD, VAN, and MER alone and in dual combinations. The PK-PD model was successfully (i) evaluated with external data from two clinical *S. aureus* isolates and further drug combinations and (ii) challenged to predict common clinical PK-PD indices and breakpoints. Finally, clinical trial simulations were performed that revealed that the combination of VAN-MER might be favorable over LZD-MER due to an unfavorable antagonistic interaction between LZD and MER.

Study Highlights

WHAT IS THE CURRENT KNOWLEDGE ON THE TOPIC?
☑ PK-PD relationships for antibiotic monotherapy have been intensely characterized. However, for combination therapies, which are increasingly administered due to suspected resistant bacteria, PK-PD characterization of antibiotic combinations is largely unexplored, even for frequently utilized combination regimens.

WHAT QUESTION DID THIS STUDY ADDRESS?
☑ The present study compared two common broad-spectrum combination therapies (i.e., either LZD or VAN combined with MER against *S. aureus*, a highly abundant infective pathogen), in a translational PK-PD framework.

WHAT THIS STUDY ADDS TO OUR KNOWLEDGE
☑ This translational PK-PD study suggests that the combination of LZD-MER might be inferior to VAN-MER against *S. aureus*. Furthermore, the study illustrates the usefulness of modeling and simulation techniques to gain insight into joint PD of antibacterial combination therapy.

HOW MIGHT THIS CHANGE DRUG DISCOVERY, DEVELOPMENT, AND/OR THERAPEUTICS?
☑ In the future, antibacterial combination therapy most probably will become even more important. Drug development programs need to adapt to this forthcoming paradigm shift by including a combined evaluation of novel drug candidates with other antibiotics already in preclinical drug development. The presented translational approach might help in planning prospective head-to-head combination trials and thus selecting the most favorable combinations for clinical evaluation. Hence, extension of the approach to further drug classes and scenarios might be useful.

Bacterial resistance to antibiotics is rising, particularly in the clinical setting.[1] Hence, nosocomial infections often require broad-spectrum antibacterial coverage, which is achieved by empiric antibiotic combination therapy. These regimens frequently include linezolid (LZD) or vancomycin (VAN), and there is an ongoing debate as to which of these drugs has more favorable properties in the clinical setting.[2] We aimed to approach this controversy from the perspective of their use in combinatory regimens. Frequently, LZD or VAN, both displaying sole gram-positive activity, are combined with meropenem (MER) to ascertain gram-negative coverage. Although resistant pathogens are often suspected in a clinical setting, methicillin-susceptible *Staphylococcus aureus* (MSSA) will turn out as an infective organism in most cases as the causative pathogen.[3]

Clinical assessment of single and combined antibacterial effects is challenging due to a lack of direct clinical readouts of the antibacterial effects. Pharmacokinetic-pharmacodynamic (PK-PD) modeling has been proven useful to link preclinical information to clinical information to comprehensively assess antibacterial effects and place them in a clinical context.[4] The *in vitro*-based PK-PD

[1]Department of Clinical Pharmacy and Biochemistry, Institute of Pharmacy, Freie Universitaet Berlin, Berlin, Germany; [2]Institute of Mathematics, University of Potsdam, Potsdam-Golm, Germany. *Correspondence: C Kloft (charlotte.kloft@fu-berlin.de)

models have also been shown to predict PK-PD indices from *in vivo* studies,[5] corroborating the translational value of *in vitro* information.

The objective of the present study was to characterize and compare antibiotic combinations of either LZD-MER or VAN-MER in a translational framework exploiting preclinical *in vitro* experiments.[6] We aimed to (i) develop a semi-mechanistic PK-PD model that predicts the individual and combined effects of LZD, VAN, and MER by accounting for the respective mechanisms of action, (ii) externally validate the PK-PD model with other MSSA isolates and drug combinations from other drug classes, (iii) assess the translational validity of the developed model by predicting PK-PD breakpoints and comparison to the clinical PK-PD indices, and (iv) link the developed semimechanistic mathematical model to published clinical population PK models to assess the consequences of combining either LZD or VAN with MER against MSSA.

METHODS
PK-PD model-building dataset
The dataset for PK-PD model-building was previously published.[6] Briefly, MSSA ATCC 29213 was exposed over 24 hours to static concentrations of LZD (0.5–32 mg/L), MER (0.015–8 mg/L), and VAN (0.06–16 mg/L) alone and in selected combinations covering the clinically relevant concentration range of the drugs.[7–9] Samples from more than or equal to two independent replicates per concentration tier were taken using a dense sampling scheme ($n \geq 8$); drug concentrations were quantified by a validated assay[10] and MSSA as colony forming units (CFU)/mL.

Semimechanistic PK-PD model building
A simplified life-cycle model[11] was utilized as the core of the PD model, which consisted of two bacterial growth states: bacteria in the growing state ("GRO") transferred into the replicating state ("REP"). In "REP," bacteria replicated ("doubling") and transferred back to "GRO." The first-order rate-constant k_{rep} was assumed to be rate-limiting and actual replication was assumed to be very fast (k_{doub} fixed to 100 h^{-1}). Bacteria being not susceptible to antibiotic exposure and not replicating ("persisters") were assumed to be generated during replication and quantified in a compartment with nonreplicating persisting bacteria,[12] ("PER"). The differential equations initialized for "GRO" with the bacterial concentration at t = 0 (CFU$_0$) as initial condition (IC) was as follows:

$$\frac{dGRO}{dt} = -k_{rep} \times GRO + k_{doub} \times REP \times 2 \quad IC = CFU_0 \quad (1)$$

$$\frac{dREP}{dt} = k_{rep} \times GRO - k_{doub} \times REP - k_{per} \times REP \quad IC = 0 \quad (2)$$

$$\frac{dPER}{dt} = k_{per} \times REP - k_{death,per} \times PER \quad IC = 0 \quad (3)$$

Drug effects were implemented by sigmoidal maximum effect models on the respective turnover rate constants in the simplified bacterial life-cycle (i.e., maximum effect (E$_{max}$), EC$_{50}$ as the concentration stimulation 50% of E$_{max}$,

and a Hill coefficient capturing the steepness of the concentration-effect relationships. The E$_{max}$ was estimated (relative to 1.0) only if more than one drug altered a rate constant and the magnitude of perturbation between those was significantly different.

$$E = E_{max} \times \frac{c^{Hill}}{EC_{50}^{Hill} + c^{Hill}} \quad (4)$$

The life-cycle model structure allowed for implementing the drug effects in various ways. Inhibition of the rate constant k_{rep} leads to purely bacteriostatic drug effects. Inhibition of k_{doub} leads to a replication-dependent drug effect with a maximum killing rate determined by the replication rate. A replication-independent drug effect is achieved by introducing a killing rate on "GRO" or "PER" to kill growing or persisting bacteria. The drug effects of LZD, VAN, and MER were implemented in different ways, as outlined above, guided by their mechanism of action and model selection criteria, as outlined below.

Potential adaptive resistance (AR) of the bacteria leading to regrowth after initial killing was implemented by an adaption submodel.[13,14] The degree of adaption was assumed to increase EC$_{50}$ over time as a function of drug exposure c(t) and a second-order time-delay rate constant τ:

$$\frac{dAR_{off}}{dt} = -\tau \times c(t) \times AR_{off} \quad IC = 1 \quad (5)$$

$$\frac{dAR_{on}}{dt} = \tau \times c(t) \times AR_{off} \quad IC = 0 \quad (6)$$

The hypothetic amount transferred to AR$_{on}$ was then multiplied by β to account for the magnitude of the adaption resulting in an adaption factor α, that ultimately scaled the EC$_{50}$ over time[14]:

$$EC_{50}(t) = \alpha(t) \times EC_{50} \quad with \quad \alpha(t) = 1 + \beta \times AR_{on}(t) \quad (7)$$

Potential interactions on the adaption level (i.e., if drug A had an influence on the adaption of the bacteria to drug B), was explored by an inhibitory effect (E$_{max}$ model) of drug A on τ of drug B and/or vice versa.

Data analysis
The "R" software program version 3.1.1 (R Core Team, Vienna, Austria) was utilized as the analysis platform for modeling and simulations. Differential equations were solved using the 'R' package "deSolve."[15] There were 1,617 timed CFU data points available for analysis of the model-building dataset. Experimentally determined as well as model-predicted CFU/mL were log-transformed for parameter estimation ('R' package "optim") using ordinary least-squares with an additive residual variability component. As experimental variability between replicates was small, no other variability components were required. Model performance was investigated by visual inspection of goodness-of-fit and visual predictive check plots (stratified by scenario). For discrimination between nested models, a significant difference in favor of the more complex model was assumed if the Δ2-fold log-likelihood (Δ-2LL) estimator

was ≥ 3.84 ($\alpha \leq 0.05$; df = 1). For non-nested model comparison, the Akaike criterion[16] was used. The precision of the parameters of the final mathematical model was assessed by a nonparametric bootstrap analysis ($n = 1,200$), in which the raw data of the time-kill curve of an experimental setting was resampled without stratification.

EXTERNAL MODEL EVALUATION
Cross-strain prediction
In order to assess if the developed PK-PD model was predictive also for other MSSA strains than the reference isolate ATCC 29213 (MIC values: LZD = 2.0 mg/L; MER = 0.125 mg/L; and VAN = 1.0 mg/L), we used time-kill curve data from two clinical isolates of MSSA,[6] MV13391 (MIC values: LZD = 2.0 mg/L; MER = 0.125 mg/L; and VAN = 1.0 mg/L) and MV13488 (MIC values: LZD = 2.0 mg/L; MER = 0.0625 mg/L; and VAN = 1.0 mg/L), which originated from tracheal secretion and sputum, respectively. We used the developed PK-PD model with its final parameter estimates to predict the time-kill curves obtained with these two clinical MSSA isolates. No parameters apart from k_{rep}, CFU_0, and CFU_{max} were altered for this purpose.

Cross-combination prediction with a focus on PD interaction patterns
As the model-building dataset[6] contained combinations between bacteriostatic and bactericidal agents, we evaluated if the developed PK-PD model was also able to predict antibacterial effects of such combinations from published time-kill curve studies, including LZD and VAN,[17] erythromycin and penicillin,[18] and chloramphenicol and ampicillin.[19] In particular, we aimed to assess whether the developed model of the present work can predict the antagonistic interactions, which were observed with the above-mentioned combinations. Time-kill curve data from these publications were digitalized using GraphClick version 3.0 (Arizona-software, Zurich/Switzerland). Due to the sparseness of these published datasets, no exposure response parameters could be estimated from the data. Hence, EC_{50} values of the semimechanistic PK-PD model were set to the respective minimal inhibitory concentration (MIC) of the antibiotics as a proxy of the drugs potency. It should be noted that the MIC does not equal EC_{50}, but its precise value has less of importance when predicting pure inhibitory concentrations above the MIC as in the external data. Further, CFU_0, CFU_{max}, and k_{rep} were estimated from the respective growth control curves. The maximum drug effects were either a result of the growth-curve for drugs exhibiting replication-dependent killing (i.e., VAN, penicillin, and ampicillin) or were adapted to drugs that exhibit replication-independent killing (i.e., LZD, erythromycin, and chloramphenicol). The persister development rate k_{per} was set to the final parameter estimate of MER, also due to the lack of data.

Prediction of PK-PD indices and breakpoints
The translational predictivity of the developed semimechanistic mathematical PK-PD model was investigated by simulating a dose fractionation study.[5] Therefore, published human population PK models of MER,[20] LZD,[21] and VAN[22] were utilized and linked to the developed semimechanistic

PK-PD model. Covariates of the population PK models were set to 35 years for age, 75.0 kg for total body weight, and 120 mL/min for creatinine clearance. Plasma protein binding was set to 2% (MER),[23] 32.8% (VAN),[24] and 13.4% (LZD).[25] Six to 10 dose levels were empirically chosen to cover concentrations around the MIC of MSSA and ranged from 80–1,200 mg (LZD), 2.5–20 mg (MER), and 10–200 mg (VAN). These doses were administered 1–12 (MER) and 1–6 times (LZD and VAN) over a simulation period of 24 hours. CFU/mL over time were predicted with the linked PK-PD model. A bactericidal effect was concluded if bacterial counts were reduced $\geq 3 \log_{10}$ CFU/mL compared to the initial inoculum; a reduction of bacteria ranging from 0–3 $\log_{10}$ CFU/mL was referred to as bacteriostatic. PK-PD indices[26] were calculated from the simulated time-kill curves and included: $\%fT_{>MIC}$ = the percentage of time that unbound drug concentrations exceed the MIC in a 24-hour period; fC_{max}/MIC = the peak unbound drug concentration divided by the MIC; and $fAUC/MIC$ = the area under the unbound concentration-time profile divided by the MIC in a 24-hour period. Breakpoints for bacteriostatic and bactericidal activity were determined according to nonlinear regression analysis and evaluated graphically and based on the coefficient of determination (R^2).

Clinical trial simulation
To explore the antibiotic effects of LZD, MER, and VAN, alone and in dual combinations, clinically utilized dosing regimens were used for simulations with the linked population PK-PD model. For simplicity, all drugs were administered as intravenous infusions over 1 hour to mimic a common clinical situation. The exploratory scenarios were LZD 600 mg b.i.d.,[27] MER 1,000 mg t.i.d.,[23] and VAN 1,000 mg b.i.d.[28] alone and in dual combinations of LZD/MER and VAN/MER. One thousand virtual patients were simulated and their covariates, age, body weight, and serum creatinine were sampled from log-normal distributions with geometric mean values of 75 kg, 35 years, and 1.0 mg/dL, respectively. An SD of 10% CV was used for all covariates. Sex and likelihood of liver cirrhosis (Child Pugh grade C) were simulated from binomial distributions with probabilities of 50% female and 5% liver cirrhosis. Creatinine clearance was subsequently calculated from those "primary" patient covariates using the Cockcroft-Gault equation.[29] The (unexplained) interindividual variability on the population PK model and uncertainty of the parameters of the semimechanistic PD model was considered by using stochastic simulations[30]: PK parameters were sampled from the respective log-normal distributions of each PK parameter for each individual virtual patient. Uncertainty of the PD model parameter estimates was considered by sampling from the obtained variance-covariance matrix of the final semimechanistic PK-PD model. Differences in bacterial susceptibility were considered by sampling MIC values from the respective EUCAST distribution (www.mic. eucast.org) for LZD, VAN, and MER (**Supplementary Figure S1**). The sampled MIC values were used to scale the active concentrations of LZD, VAN, and MER in the semimechanistic PK-PD model (i.e., $C_{active\ drug} = C_{drug}/MIC_{EUCAST}/MIC_{ATCC29213}$). Time-courses of CFU/mL of the
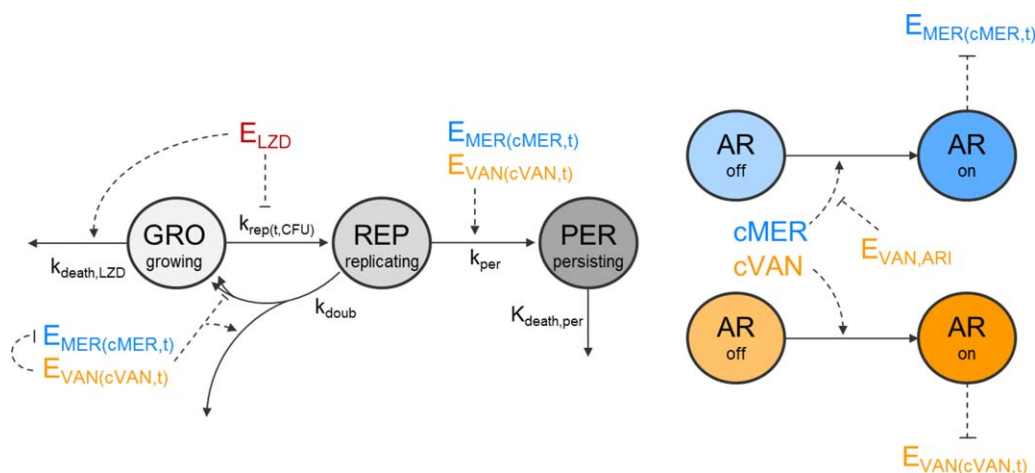
Figure 1 Graphical sketch of the semimechanistic pharmacodynamic model (left) and adaption submodel of vancomycin (VAN) and meropenem (MER) (right) for lag-phase *Staphylococcus aureus* (*S. aureus*); solid arrows = mass transfer between compartments; dashed arrows = stimulatory effects; ⎯l: inhibitory effects. AR, adaptive resistance; CFU, colony forming unit; GRO, growing state; LZD, linezolid; PER, persisting bacteria; REP, replicating state.

different regimens were predicted over 24 hours and compared between the different therapies.

RESULTS
Semimechanistic PK-PD model
The final semimechanistic PD model that simultaneously described the single and combined effects of LZD, MER, and VAN against MSSA is illustrated in **Figure 1**, and consisted of the following system of ordinary differential equations:

$$\frac{dGRO}{dt} = -k_{death,LZD} \times E_{LZD} \times GRO - k_{rep}(t, CFU) \times (1 - E_{LZD}) \times GRO$$
$$+ k_{doub} \times [1 - E_{MER} \times (1 - Emax_{MER,Eagle} \times E_{MER,Eagle}) \times (1 - E_{VAN})]$$
$$\times (1 - Emax_{VAN} \times E_{VAN}) \times REP \times 2 \quad IC = CFU_0$$

$$(8)$$

$$\frac{dREP}{dt} = k_{rep}(t, CFU) \times (1 - E_{LZD}) \times GRO - k_{doub} \times REP$$
$$- k_{per,MER} \times E_{MER} \times REP - k_{per,VAN} \times E_{VAN} \times REP \quad IC = 0 \quad (9)$$

$$\frac{dPER}{dt} = k_{per,MER} \times E_{MER} \times REP + k_{per,VAN} \times E_{VAN} \times REP$$
$$- k_{death,PER} \times PER \quad IC = 0 \quad (10)$$

k_{rep} was assumed to decrease asymptotically to zero if bacterial concentrations reached the capacity limit CFU_{max}. The lag-phase to attain exponential growth, as seen in GC in **Figure 2**, was estimated by a first-order delay rate constant k_{lag}. Both aspects were considered as follows:

$$k_{rep}(t, CFU) = k_{rep} \times (1 - e^{-k_{lag}t}) \times \left(1 - \frac{GRO + REP + PER}{CFU_{max}}\right) \quad (11)$$

MER and VAN, as cell wall-active antibiotics, impaired successful doubling causing loss of bacteria entering replication "REP." MER alone fully inhibited doubling (i.e., E_{max}

of 100% on k_{doub}) at optimal concentrations up to 0.5 mg/L and to only 67.2% at higher concentrations up to 8 mg/L (so-called paradoxical "Eagle-effect," cf. M4 vs. M64 in **Figure 2**). This paradoxical effect was implemented as an inhibitory effect on the drug effect of MER occurring at higher concentrations, which considerably improved the model ($\Delta AIC = -104.64$). VAN alone impaired successful doubling of the bacteria to 74.3% (cf. compare the lower killing rate of VAN to MER at optimal concentrations; e.g., V16 vs. M4 in **Figure 2**). The concentration-effect relationship of initial killing of VAN (cf. V0.5 vs. V0.75 in **Figure 2**) was very steep and estimation of the Hill factor H was imprecise; hence, H for VAN was fixed to 20, as in previous studies.[12] The joint effects of VAN and MER were implemented by an empirical modified Bliss Independence term $(1-E_{MER}) \times (1-E_{VAN})$, accounting for the self-inhibitory Eagle effect of MER and the observation that the maximum joint effect of MER and VAN was limited to the effect of VAN (cf. M4 vs. V4M4 in **Figure 2**). Both VAN and MER simulated drug-unsusceptible persisting bacteria (quantified in "PER") after initial killing (cf. M2 and V4), being quantified in "PER," whose inclusion was highly significant for MER (Δ-2LL = -64.89) and VAN (Δ-2LL = -47.8).

LZD, as a protein synthesis inhibitor, inhibited transition of the bacteria into the replicating state "REP." Hence, bacteria were growth-arrested in "GRO" in the presence of LZD and only a replication-independent killing of bacteria was observed ($k_{death,LZD}$; e.g., as apparent in L16 in **Figure 2**). When MER was combined with LZD, growth-arrested bacteria were protected from the replication-dependent effect of MER and the combined effect corresponded to the effect of LZD alone explaining the antagonism between LZD and MER in a mechanistic fashion (cf. M4 vs. L4 vs. L4M4 in **Figure 2**).

Both MER and VAN showed significant degradation during the time-kill curve study to 62.9% and 90.6% of their concentration at t = 0, respectively[10]: drug degradation was considered in the PK-PD model by implementing first-order
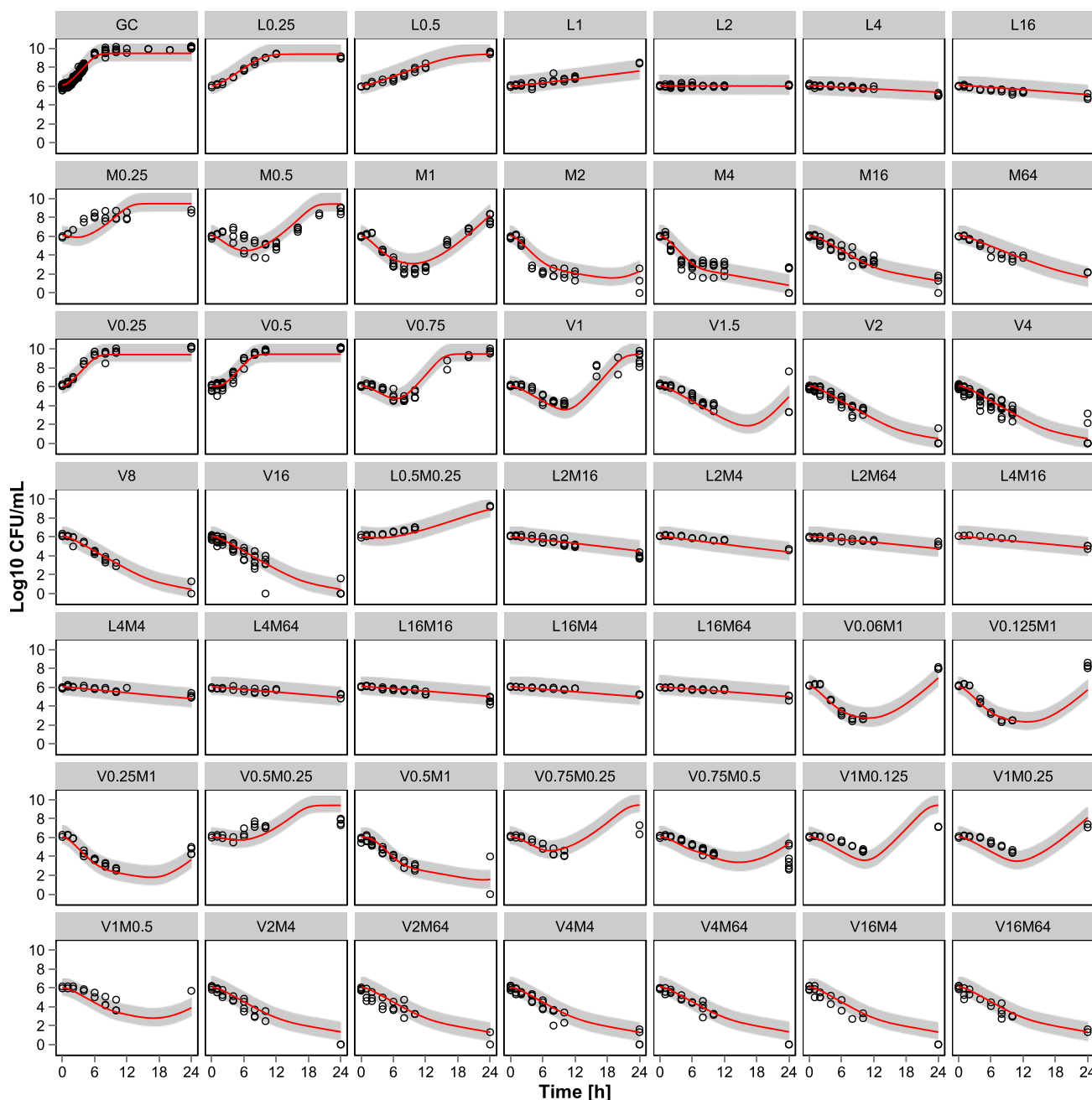
Figure 2 Visual predictive check plots for the final semimechanistic pharmacodynamic model for methicillin-susceptible Staphylococcus aureus ATCC 29213. Points represent experimental data; the red line indicates median prediction and the gray shaded area represents the 90% prediction intervals based on 1,000 stochastic simulations for each scenario. Lx/Mx/Vx = multiples/fractions of the minimum inhibitory concentration of linezolid, meropenem, and vancomycin, respectively. CFU, colony forming unit.

degradation rate constants of 0.019 h^{-1} for MER and 0.0039 h^{-1} for VAN, respectively, on the initial drug concentration. Yet, degradation alone was not sufficient to explain the observed regrowth after initial killing for MER and VAN at concentrations around their MIC values (cf. M1 and V1 in **Figure 2**). The adaption process was assumed to occur on the level of EC$_{50}$ using an adaption model from Tam *et al.*[14] formulated as system of ordinary differential equations:

$$\frac{dAR_{off,\ VAN}}{dt} = -\tau \times C_{VAN}(t) \times AR_{VAN,off} \quad \text{IC} = 1 \tag{12}$$

$$\frac{dAR_{on,VAN}}{dt} = \tau \times C_{VAN}(t) \times AR_{VAN,off} \quad \text{IC} = 0 \tag{13}$$

$$EC_{50,VAN}(t) = \alpha_{VAN}(t) \times EC_{50,VAN,t=0} \quad \text{with} \quad \alpha_{VAN}(t) = 1 + \beta_{VAN} \times AR_{on,VAN}(t) \tag{14}$$

Table 1 Parameter estimates of the final semimechanistic PD model for MSSA ATCC 29213

Parameter [unit]	Estimate	RSE % [95% CI]	Explanation
Parameters of the bacterial life-cycle			
CFU_0 [$\log_{10}$ CFU/mL]	6.06	0.4 [6.02–6.09]	Initial CFUs/mL at beginning of the experiment
CFU_{max} [$\log_{10}$ CFU/mL]	9.43	0.6 [9.26–9.68]	Maximum attainable bacterial growth
k_{lag} [h^{-1}]	0.88	16.0 [0.662–2.28]	First-order time delay rate constant to attain log-phase
k_{rep} [h^{-1}]	1.56	7.2 [1.25–1.90]	Transit rate constant from growing to replicating state; rate-limiting step for growth
k_{doub} [h^{-1}]	100	FIX [-]	Rate constant of doubling; represents actual replication (fixed to high rate constant as not rate-limiting); MER and VAN impaired successful replication
$k_{death, per}$ [h^{-1}]	0.23	9.3 [0.189–0.307]	Basal death rate constant of persistent bacteria
Drug-related parameters			
$EC_{50,LZD}$ [mg/L]	0.68	9.1 [0.563–0.802]	C_{LZD} leading to half-maximum drug effect of LZD on k_{rep} (growth arrest) and stimulation of $k_{death,LZD}$
H_{LZD} [-]	1.55	7.5 [1.35–1.63]	Hill factor LZD (steepness of the concentration-effect relationship)
$k_{death, LZD}$ [h^{-1}]	0.10	7.5 [0.092–0.114]	Basal death rate constant of growth-arrested bacteria, induced by LZD
$EC_{50,MER,t=0}$ [mg/L]	0.022	2.8 [0.0189–0.0262]	C_{MER} leading to half-maximum drug effect of MER on k_{doub} and $k_{per,MER}$ at t = 0
H_{MER} [-]	3.23	11.7 [2.27–5.48]	Hill factor MER (steepness of the concentration-effect relationship)
$Emax_{MER,Eagle}$,%	32.8	5.9 [26.2–35.6]	Percentage by which the effect of MER at higher concentration decreased from maximum (67.2% impaired doublings remained)
$EC_{50,MER,Eagle}$ [mg/L]	1.35	8.9 [0.856–1.41]	C_{MER} leading to half-maximum paradoxical effect of MER on k_{doub}
$H_{MER, Eagle}$ [-]	4	FIX [-]	Hill factor MER (steepness of the concentration Eagle-effect relationship)
β_{MER} [-]	9.53	4.2 [7.61–22.0]	Factor that calculates maximum possible adapted EC_{50} of bacteria by [$(1+\beta_{MER}) \times EC_{50,MER,t=0}$]
τ_{MER} [L/(mg·h)]	0.47	5.8 [0.154–0.653]	Second-order delay rate constant for adaption with respect to time and C_{MER}
$k_{per,MER}$ [h^{-1}]	0.11	32.6 [0.0545–0.263]	Persister development rate for MER during replication
$k_{deg,MER}$ [h^{-1}]	0.019	FIX [-]	First-order degradation rate constant of C_{MER}; drug degradation determined by HPLC, hence, fixed during estimation
$Emax_{VAN}$, %	74.3	1.9 [70.8–78.5]	Percentage by which VAN decreased successful doubling at maximum
$EC_{50,VAN,t=0}$ [mg/L]	0.46	1.8 [0.430–0.482]	C_{VAN} leading to half-maximum drug effect of VAN on k_{doub} and $k_{per,VAN}$ at t = 0
H_{VAN} [-]	20	FIX [-]	Hill factor VAN (steepness of the concentration-effect relationship); fixed as estimation was not possible and very steep (on/off) initial concentration-effect relationship was observed in time-kill curves
$EC_{50,VAN,ARI}$ [mg/L]	0.39	5.0 [0.293–0.515]	C_{VAN} leading to half-maximum suppression of adaption of MSSA to MER
$H_{,VAN,ARI}$ [-]	1.0	FIX [-]	Hill factor VAN for suppression of adaption of MSSA to MER
β_{VAN} [-]	3.59	6.7 [2.60–4.81]	Factor that calculates maximum possible adapted EC_{50} of bacteria by [$(1+\beta_{VAN}) \times EC_{50,VAN,t=0}$]
τ_{VAN} [L/(mg·h)]	0.034	11.2 [0.0197–0.0638]	Second-order delay rate constant for adaption with respect to time and C_{VAN}
$k_{per,VAN}$ [h^{-1}]	0.017	50.9 [0.00722–0.0561]	Persister development rate constant for VAN during replication
$k_{deg,VAN}$ [h^{-1}]	3.9e-03	FIX [-]	First-order degradation rate constant of C_{VAN}; drug degradation determined by HPLC, as an independent variable, was fixed during estimation
σ [$\log_{10}$ CFU/mL]	0.63	-	Residual additive variability, no RSE reported as calculated from final objective function value

CFU, colony forming unit; CI, confidence interval; EC_{50}, half-maximal effective concentration; E_{max}, maximum effect; HPLC, high-performance liquid chromatography; LZD, linezolid; MER, meropenem; MSSA, methicillin-susceptible Staphylococcus aureus; PD, pharmacodynamic; RSE, relative standard error; VAN, vancomycin.

Relative standard errors (RSE) in % obtained from the variance-covariance matrix, 95% confidence intervals determined by a non-parametric bootstrap analysis (n = 1198) and short explanation of the model parameters.
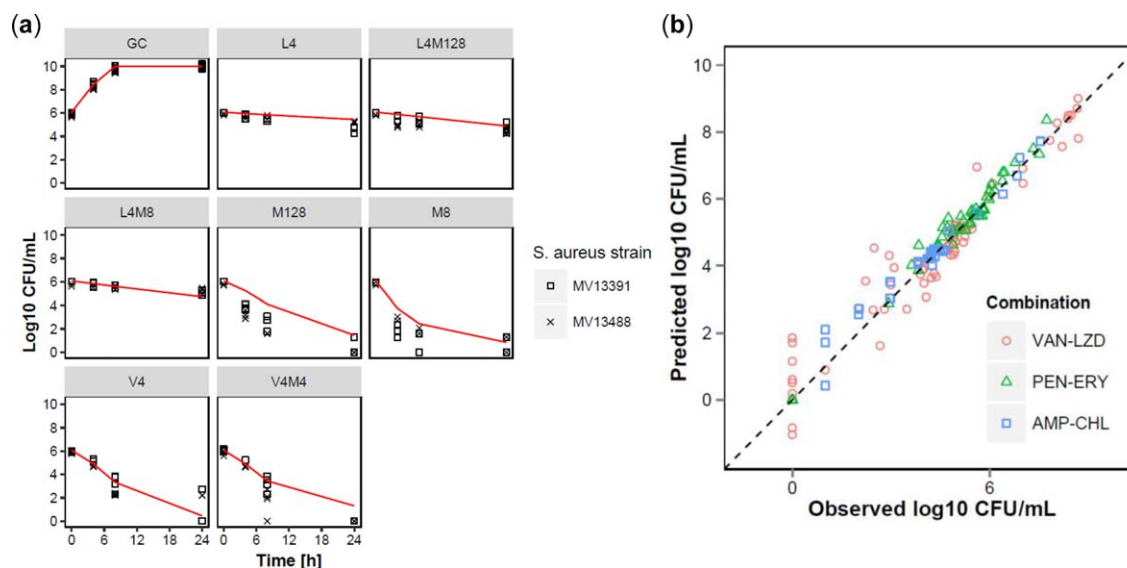
Figure 3 (**a**) External evaluation of the semimechanistic pharmacokinetic-pharmacodynamic model to predict time-kill curves of selected drug combinations of methicillin-susceptible Staphylococcus aureus (*S. aureus*) isolates MV13391 and MV13488; (**b**) observed vs. predicted log10 colony forming unit (CFU)/mL for the external evaluation for the antibiotics vancomycin (VAN) and linezolid (LZD) against methicillin-resistant *S. aureus*, penicillin (PEN) and erythromycin (ERY) against *S. pneumoniae* and ampicillin (AMP) and chloramphenicol (CHL) against group B streptococci, detailed predicted and observed time-kill curve data is presented in the **Supplementary Material**.

$$\frac{dAR_{off,\ MER}}{dt} = -\left(1 - E_{VAN,ARI}\right) \times \tau_{MER} \times C_{MER}(t) \times AR_{off,MER} \quad \text{IC} = 1$$

$$\text{(15)}$$

$$\frac{dAR_{on,MER}}{dt} = \left(1 - E_{VAN,ARI}\right) \times \tau_{MER} \times C_{MER}(t) \times AR_{off,MER} \quad \text{IC} = 0 \quad \text{(16)}$$

$$EC_{50,MER}(t) = \alpha_{MER}(t) \times EC_{50,MER,t=0} \quad \text{with} \quad \alpha_{MER}(t) = 1 + \beta_{MER} \times AR_{on,MER}(t)$$

The model also comprised a PD interaction on the adaption level ($E_{VAN,ARI}$; i.e., subinhibitory concentrations of VAN delayed the adaption of MSSA to MER), which was highly significant (Δ-2LL $= -663.20$). This can be seen in the data when inactive V0.5 is added to M1 that alone displayed bacterial regrowth, whereas V0.5M1 did not display any regrowth (**Figure 2**). Conversely, if a potential PD interaction on the adaption level between MER influencing the adaption of MSSA to VAN was evaluated, the more complex model with both adaption processes resulted in a worse model fit than the final model and also the likelihood ratio test favored the final model. This indicates a monodirectional interaction between VAN and MER on the adaption level, of which the mechanism remains to be elucidated in future studies. All PK-PD model parameters are presented in **Table 1**. The R code of the final model is presented in Code S1 in the **Supplementary Material**.

Model evaluation
The visual predictive check indicated that the final semimechanistic PK-PD model well described all experimental data (**Figure 2**). The external evaluation focusing on the cross-strain prediction indicated that the developed PK-PD model

was capable to predict the time-kill curves of a single drug or dual combinations in clinical MSSA isolates other than the reference strain ATCC 29213 that was utilized for model building (**Figure 3a**). This indicates that the antagonism between LZD and MER and the additive-to-synergistic interaction between VAN and MER is not limited to ATCC 29213, but also present in other (clinical) MSSA strains. The external evaluation focusing on prediction of combined effects of other drugs with similar mechanisms of (inter)action revealed that the developed semimechanistic PK-PD model successfully predicted antagonism between VAN, penicillin, and ampicillin as cell wall-active antibiotics and LZD, erythromycin, and chloramphenicol as protein-synthesis inhibitors (**Figure 3b**). The time courses of the predictions of the external validation are presented in the **Supplementary Figures S2–S4**.

Prediction of PK-PD indices and breakpoints
The simulated dose fractionation study displayed for MER that unbound drug concentrations above the MIC ($f\%T_{>MIC}$) correlated best with the antibacterial effect at 24 hours (**Figure 4**). If the drug concentrations exceeded the MIC over 50% or 65% of the 24-hour period, a bacteriostatic or bactericidal effect, respectively, was observed. For LZD, both $f\%T_{>MIC}$ and fAUC/MIC correlated well with the antibacterial effect and had to exceed 98% of the 24-hour period or 56, respectively, for a bacteriostatic effect. No bactericidal effect was attained. For VAN, differentiation between the investigated PK-PD indices was less distinct. For fAUC/MIC, as traditionally monitored in a clinical setting, 59 or 94 were associated with a bacteriostatic or bactericidal effect, respectively.
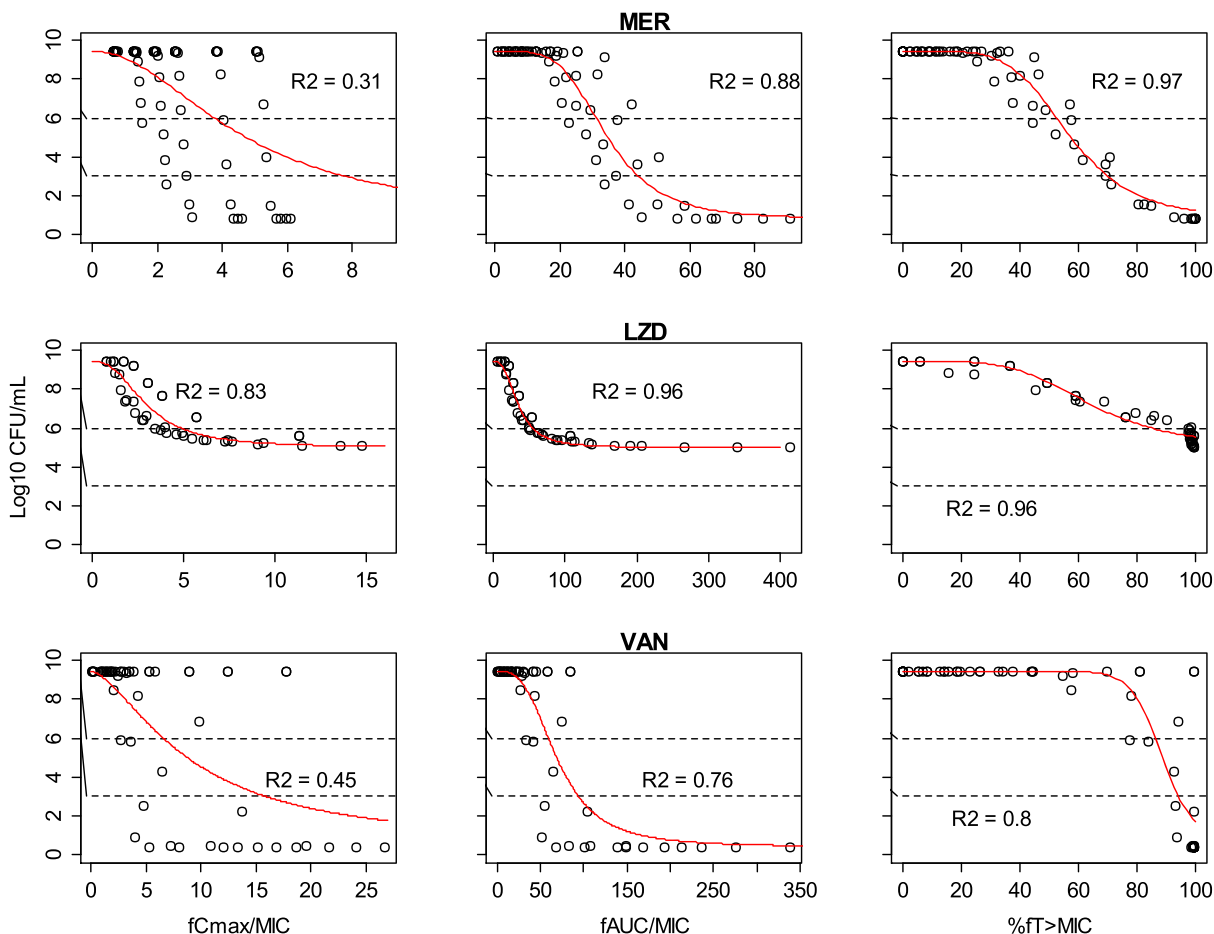
Figure 4 Prediction of pharmacokinetic-pharmacodynamic (PK-PD) indices fC_{max}/MIC (C_{max}, peak plasma concentration, MIC, minimum inhibitory concentration), $fAUC$/MIC (AUC, area under the curve), and %$fT_{>MIC}$ for meropenem (MER), linezolid (LZD), and vancomycin (VAN) against methicillin-resistant Staphylococcus aureus. Points represent simulated log10 colony forming unit (CFU)/mL at 24 hours using the linked population PK-PD model, dashed horizontal lines at 6 log10 CFU/mL represent inoculum and bacteriostatic effect, dashed horizontal line at 3 log10 CFU/mL represents bactericidal effect, red lines represent prediction of an inhibitory sigmoidal maximum effect model fitted to the simulated data, and R^2 = coefficient of determination.

Clinical trial simulation

The simulated dosing scenarios with the linked population PK-PD model are illustrated in **Figure 5**. The clinical trial simulation of MER of 1,000 mg t.i.d. in the virtual patient population resulted in unbound C_{max} was of 32.3 mgL (22.2–45.9 mg/L) in median (5th-95th percentile) (22.2–45.9 mg/L) and unbound C_{min} was 0.48 mg/L (0.018–2.76 mg/L) after the first dose (**Figure 5**). The predicted time-course of the antibacterial effect indicated that the regimen was effective against MSSA and in 88% of the virtual patients a bactericidal effect was attained at 24 hours.

For LZD, the standard regimen of 600 mg LZD b.i.d. resulted in unbound C_{max} of 11.6 mg/L in median (5th-95th percentile: 6.7818.2 mg/L) and unbound C_{min} of 4.20 mg/L in median (1.677.20 mg/L) after the first dose. This resulted only in marginal median killing to 5.3 log10 CFU/mL with a narrow effect spread (90% prediction interval (PI) = 5.0–6.3 log10 CFU/mL) after 24 hours, indicating

that, for most virtual patients, the maximum effect was attained.

VAN 1,000 mg b.i.d. resulted in unbound C_{max} of 18.2 mg/L in median (5th–95th percentile: 11.5–37.1 mg/L) and unbound C_{min} of 2.11 mg/L in median (1.14–3.92 mg/L) after the first dose. The predicted time-kill curves showed that this regimen was bactericidal in median, and after 24 hours for 84% of the virtual patients the bacterial load was lower than 3.0 log10 CFU/mL.

The combination of LZD 600 mg b.i.d. with MER 1,000 mg t.i.d. stimulated a bacteriostatic effect to a median bacterial load of 4.8 log10 CFU/mL after 24 hours (90% PI = 4.6–5.0 log10 CFU/mL), being substantially inferior to the effect of MER 1,000 mg t.i.d. alone after 24 hours (median = 1.4 log10 CFU/mL; 90% PI = 1.2–6.3 log10 CFU/mL), but slightly larger compared to LZD 600 mg b.i.d. alone after 24 hours (median = 5.3 log10 CFU/mL; 90% PI = 5.0–6.3 log10 CFU/mL).
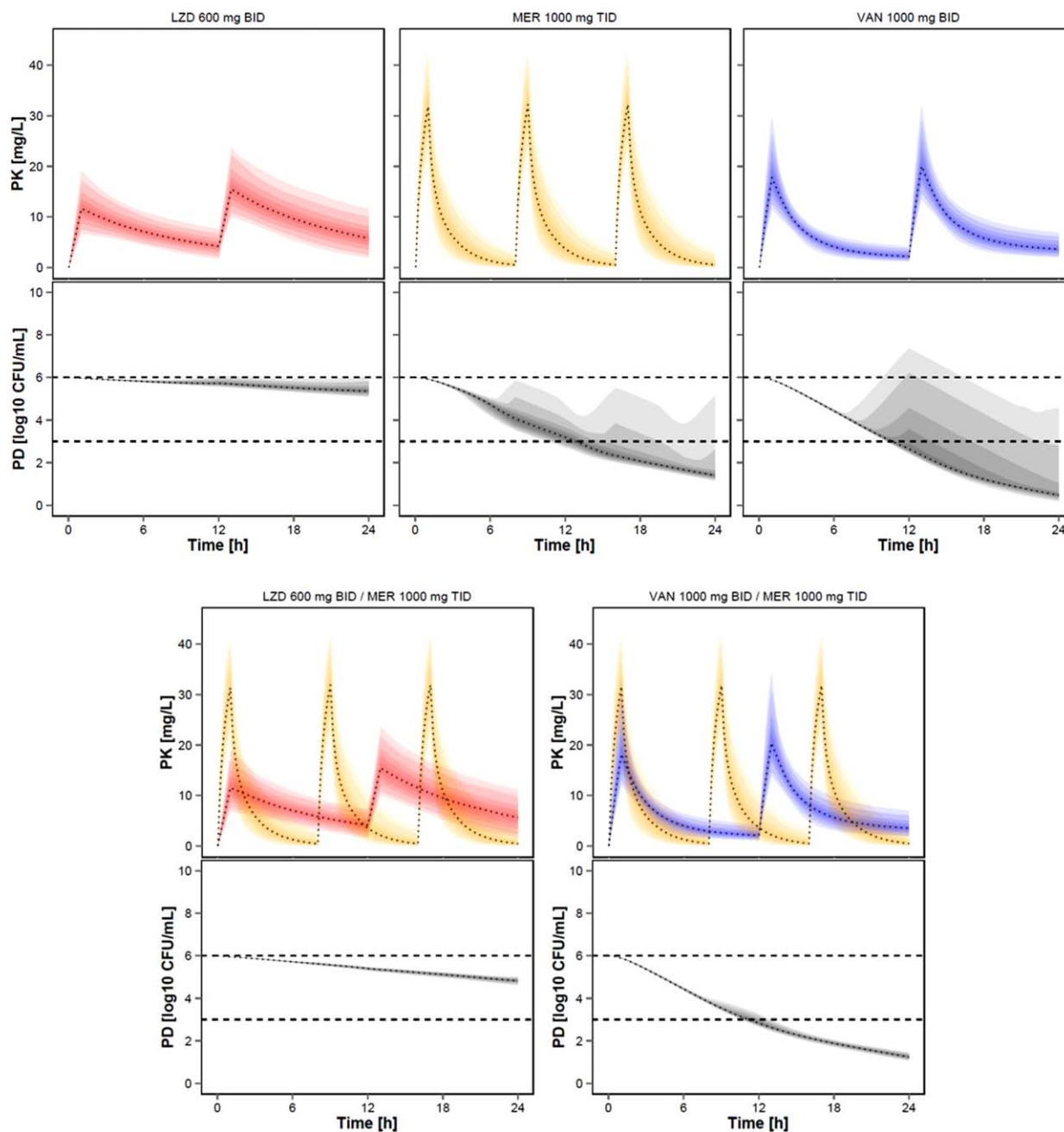
Figure 5 Predicted drug concentration and colony forming unit (CFU)/mL for methicillin-susceptible Staphylococcus aureus against a monotherapy of linezolid (LZD) 600 mg b.i.d. (red), meropenem (MER) 1,000 mg t.i.d. (yellow), and vancomycin (VAN) 1,000 mg b.i.d. (blue) or their dual MER-based combination therapies with the same dosing. Median prediction (dotted lines) of unbound drug concentrations (pharmacokinetic (PK); upper panel) and drug effect as log10 CFU/mL over time (pharmacodynamic (PD); lower panel), variability (shaded area) ranging from the 5th to the 95th percentile (20th, 40th, 60th, 80th, and 90th prediction intervals), dashed horizontal line at 6 log10 CFU/mL represents inoculum and bacteriostatic effect, dashed horizontal line at 3 log10 CFU/mL represents bactericidal effect.

The combination of VAN 1,000 mg b.i.d. with MER 1,000 mg t.i.d. resulted in a bactericidal effect at 24 hours, as observed with both antibiotics individually. However, the combinatory regimen reduced the observed interindividual variability of the antibacterial effects observed with the single antibiotic regimens (**Figure 5**) and a bacterial load of 1.3 log10 CFU/mL (90% PI = 1.1–1.5 log10 CFU/mL) was attained at 24 hours.

DISCUSSION

The present study compared the commonly used combination therapies LZD-MER and VAN-MER in a translational framework exploiting preclinical *in vitro* studies. By linking the developed semimechanistic PK-PD model based upon preclinical information to clinical population PK data of the three antibiotics, we could translate single and combined

effects of LZD, VAN, and MER into a clinical perspective: MER and VAN alone displayed considerably rapid bactericidal activity for most of the virtual patients. The predictions for LZD alone indicated only a bacteriostatic effect. The combination of MER and VAN displayed an additive interaction and subinhibitory concentrations of VAN even prevailed the AR development of MER leading to an overall higher rate of bactericidal activity compared to each drug alone. The combination of LZD and MER displayed an unfavorable interaction and the bactericidal effect of MER alone was antagonized to bacteriostasis with only marginal bacterial killing. In clinical situations when bactericidal activity is deemed favorable (e.g., infections in neutropenic patients or in treating endocarditis),[31] clinicians should be watchful when applying the combination MER-LZD and may consider MER-VAN in these cases.

PK-PD modeling has proven to be a useful tool to comprehensively and systematically evaluate combination therapies,[32,33] which is difficult to perform in a pure clinical setting due to resource or ethical constraints. To be able to capture replication dependent and independent drug effects, we used a simplified blueprint of the bacterial life cycle[11] for simultaneously modeling of the single and combined effects. The life-cycle model enabled to include the drug effects motivated by their respective mode of action. As cell wall-active antibiotics, MER and VAN were assumed to exert a replication-dependent effect (i.e., perturbation of successful doubling), whereas LZD, as a protein-synthesis inhibitor, inhibited the transition into the replicating state. Thereby, the antagonism between LZD and MER was already intrinsically implemented as the effect of LZD growth-arrested the bacterial life-cycle and, thus, precluded the effect of MER. The combined effects of VAN and MER were implemented as an inhibitory replication-dependent effect, reducing the percentage of successful doublings according to a modified Bliss Independence term.[34,35] The core of this term, $(1-E_{MER})\times(1-E_{VAN})$, was extended to account for the observed deviations from conventional Bliss Independence, including the inferior maximum effect of VAN compared to MER, the paradoxically reduced "Eagle-effect"[36] at higher concentrations observed for MER, and the VAN-limited combined effect of combinations of VAN and MER.

The developed semimechanistic PK-PD model in the present study was successfully evaluated with external data for prediction into other clinical MSSA strains, supporting the generalizability of our results in MSSA-related infections. Moreover, the semimechanistic PK-PD model was capable to predict further antagonistic interactions from a larger number of published studies indicating that the structural PK-PD model can be also applied to further drug combinations of bacteriostatic and bactericidal drugs. Last, we also assessed the relation of the semimechanistic PK-PD model to typically utilized PK-PD indices and breakpoints that are used in a clinical setting. For LZD, the determined value of 56 for *f*AUC/MIC in the present work is fairly close to the breakpoints in animals (AUC/MIC of 83)[37] and humans (AUC/MIC of 51–85)[38] for bloodstream infections if protein binding is considered. For MER, the determined value of 52% *f*%T$_{>MIC}$ was also in good agreement with

the clinical breakpoint for microbiological response of 54% determined in patients with lower respiratory tract infections, in which *S. aureus* was the second-most abundant pathogen.[39] For VAN, the *f*AUC/MIC breakpoints from the clinical studies[40,41] tended to be fairly higher (125–400) than the calculated values (59–94) of the present work, which could originate from the partly impaired tissue distribution of VAN,[42] whereas for MER and LZD, unbound plasma concentrations might be a fair predictor of tissue concentrations,[43–45] if determined under appropriate analytic conditions.[24,46,47] Yet, the overall "correct" prediction of the PK-PD index indicates that the developed semimechanistic PK-PD model might adequately reflect the clinical situation for the antibiotics LZD, MER, and VAN and, hence, might support the validity of the drawn conclusions from the present translational study. For future studies, it might be valuable to explore the combined drug effects of LZD, MER, and VAN in scenarios that are longer than 24 hours. In particular, addition of dynamic time-kill curve data from, for example, hollow-fiber experiments might be valuable to provide insight into persistent drug effects, including potential interactions on these. The present model could aid in the optimal design of such experiments.

CONCLUSION

The present study compared two common empiric broad-spectrum antibacterial regimens consisting of LZD-MER and VAN-MER against MSSA as the highest-abundant pathogen in many infections. Using preclinical *in vitro* data studies combined with clinical population PK data of the antibiotics, we could evaluate these regimens in a translational approach with a comprehensively evaluated semimechanistic PK-PD model. If bactericidal activity is warranted, clinicians may favor the combination of VAN-MER over LZD-MER due to the unfavorable and likely clinically relevant antagonistic interaction between LZD and MER.

1. WHO Antimicrobial Resistance Global Report on Surveillance. <http://www.who.int/drugresistance/documents/surveillancereport/en/> (2014).
2. Wunderink, R.G. *et al.* Linezolid in methicillin-resistant Staphylococcus aureus nosocomial pneumonia: a randomized, controlled study. *Clin. Infect. Dis.* **54**, 621–629 (2012).
3. European antimicrobial resistance surveillance system susceptibility of staphylococcus aureus isolates to methicillin in participating countries in 2012. <http://www.ecdc.europa.eu/en/healthtopics/antimicrobial_resistance/database/Pages/table_reports.aspx> (2012).
4. Nielsen, E.I. & Friberg, L.E. Pharmacokinetic-pharmacodynamic modeling of antibacterial drugs. *Pharmacol. Rev.* **65**, 1053–1090 (2013).
5. Nielsen, E.I., Cars, O. & Friberg, L.E. Pharmacokinetic/pharmacodynamic (PK/PD) indices of antibiotics predicted by a semimechanistic PKPD model: a step toward model-based dose optimization. *Antimicrob. Agents Chemother.* **55**, 4619–4630 (2011).
6. Wicha, S.G., Kees, M.G., Kuss, J. & Kloft, C. Pharmacodynamic and response surface analysis of linezolid or vancomycin combined with meropenem against Staphylococcus aureus. *Pharm. Res.* **32**, 2410–2418 (2015).

7. MacGowan, A.P. Pharmacokinetic and pharmacodynamic profile of linezolid in healthy volunteers and patients with Gram-positive infections. *J. Antimicrob. Chemother.* **51** Suppl 2, ii17-ii25 (2003).

8. Nicolau, D.P. Pharmacokinetic and pharmacodynamic properties of meropenem. *Clin. Infect. Dis.* **47** (suppl. 1), S32–S40 (2008).

9. Lamer, C. *et al.* Analysis of vancomycin entry into pulmonary lining fluid by bronchoalveolar lavage in critically ill patients. *Antimicrob. Agents Chemother.* **37**, 281–286 (1993).

10. Wicha, S.G. & Kloft, C. Simultaneous determination and stability studies of linezolid, meropenem and vancomycin in bacterial growth medium by high-performance liquid chromatography. *J. Chromatogr. B Analyt. Technol. Biomed. Life Sci.* **1028**, 242–248 (2016).

11. Bulitta, J.B., Ly, N.S., Yang, J.C., Forrest, A., Jusko, W.J. & Tsuji, B.T. Development and qualification of a pharmacodynamic model for the pronounced inoculum effect of ceftazidime against Pseudomonas aeruginosa. *Antimicrob. Agents Chemother.* **53**, 46–56 (2009).

12. Nielsen, E.I., Viberg, A., Löwdin, E., Cars, O., Karlsson, M.O. & Sandström, M. Semi-mechanistic pharmacokinetic/pharmacodynamic model for assessment of activity of antibacterial agents from time-kill curve experiments. *Antimicrob. Agents Chemother.* **51**, 128–136 (2007).

13. Mohamed, A.F., Nielsen, E.I., Cars, O. & Friberg, L.E. Pharmacokinetic-pharmacodynamic model for gentamicin and its adaptive resistance with predictions of dosing schedules in newborn infants. *Antimicrob. Agents Chemother.* **56**, 179–188 (2012).

14. Tam, V.H., Schilling, A.N. & Nikolaou, M. Modelling time-kill studies to discern the pharmacodynamics of meropenem. *J. Antimicrob. Chemother.* **55**, 699–706 (2005).

15. Soetaert, K., Petzoldt, T. & Setzer, R.W. Solving differential equations in R. *R J.* **2**, 5–15 (2010).

16. Akaike, H. A new look at the statistical model identification. *IEEE Trans. Automat. Contr.* **19**, 716–723 (1974).

17. Singh, S.R., Bacon, A.E. 3rd, Young, D.C. & Couch, K.A. In vitro 24-hour time-kill studies of vancomycin and linezolid in combination versus methicillin-resistant Staphylococcus aureus. *Antimicrob. Agents Chemother.* **53**, 4495–4497 (2009).

18. Johansen, H.K., Jensen, T.G., Dessau, R.B., Lundgren, B. & Frimodt-Moller, N. Antagonism between penicillin and erythromycin against Streptococcus pneumoniae in vitro and in vivo. *J. Antimicrob. Chemother.* **46**, 973–980 (2000).

19. Weeks, J.L., Mason, E.O. Jr, & Baker, C.J. Antagonism of ampicillin and chloramphenicol for meningeal isolates of group B streptococci. *Antimicrob. Agents Chemother.* **20**, 281–285 (1981).

20. Li, C., Kuti, J.L., Nightingale, C.H. & Nicolau, D.P. Population pharmacokinetic analysis and dosing regimen optimization of meropenem in adult patients. *J. Clin. Pharmacol.* **46**, 1171–1178 (2006).

21. Sasaki, T. *et al.* Population pharmacokinetic and pharmacodynamic analysis of linezolid and a hematologic side effect, thrombocytopenia, in Japanese patients. *Antimicrob. Agents Chemother.* **55**, 1867–1873 (2011).

22. Llopis-Salvia, P. & Jiménez-Torres, N.V. Population pharmacokinetic parameters of vancomycin in critically ill patients. *J. Clin. Pharm. Ther.* **31**, 447–454 (2006).

23. Astra Zeneca Meronem - Fachinformation. <https://www.astrazeneca.com/country-sites/switzerland/products.html> (2011).

24. Kees, M.G., Wicha, S.G., Seefeld, A., Kees, F. & Kloft, C. Unbound fraction of vancomycin in intensive care unit patients. *J. Clin. Pharmacol.* **54**, 318–323 (2014).

25. Buerger, C., Plock, N., Dehghanyar, P., Joukhadar, C. & Kloft, C. Pharmacokinetics of unbound linezolid in plasma and tissue interstitium of critically ill patients after multiple dosing using microdialysis. *Antimicrob. Agents Chemother.* **50**, 2455–2463 (2006).

26. Mouton, J.W., Dudley, M.N., Cars, O., Derendorf, H. & Drusano, G.L. Standardization of pharmacokinetic/pharmacodynamic (PK/PD) terminology for anti-infective drugs: an update. *J. Antimicrob. Chemother.* **55**, 601–607 (2005).

27. Pfizer ZYVOXID - German summary of product characteristics (Fachinformation). <http://www.medicines.org.uk/emc/medicine/9857> (2011).

28. Riemser Arzneimittel AG Vancomycin 'Lederle'- German summary of product characteristics (Fachinformation). <http://docplayer.org/20817140-Fachinformation-riemser-vancomycin-lederle-500-1000.html> (2003).

29. Cockcroft, D.W. & Gault, M.H. Prediction of creatinine clearance from serum creatinine. *Nephron* **16**, 31–41 (1976).

30. Metropolis, N. & Ulam, S. The Monte Carlo method. *J. Am. Stat. Assoc.* **44**, 335–341 (1949).

31. Finberg, R.W. *et al.* The importance of bactericidal drugs: future directions in infectious disease. *Clin. Infect. Dis.* **39**, 1314–1320 (2004).

32. Ly, N.S. *et al.* Colistin and doripenem combinations against Pseudomonas aeruginosa: profiling the time course of synergistic killing and prevention of resistance. *J. Antimicrob. Chemother.* **70**, 1434–1442 (2015).

33. Mohamed, A.F., Kristoffersson, A.N., Karvanen, M., Nielsen, E.I., Cars, O. & Friberg, L.E. Dynamic interaction of colistin and meropenem on a WT and a resistant strain of Pseudomonas aeruginosa as quantified in a PK/PD model. *J. Antimicrob. Chemother.* **71**, 1279–1290 (2016).

34. Bliss, C.I. The toxicity of poisons applied jointly. *Ann. Appl. Biol.* **26**, 585–615 (1939).

35. Fitzgerald, J.B., Schoeberl, B., Nielsen, U.B. & Sorger, P.K. Systems biology and combination therapy in the quest for clinical efficacy. *Nat. Chem. Biol.* **2**, 458–466 (2006).

36. Eagle, H. & Musselman, A.D. The rate of bactericidal action of penicillin in vitro as a function of its concentration, and its paradoxically reduced activity at high concentrations against certain organisms. *J. Exp. Med.* **88**, 99–131 (1948).

37. Andes, D., van Ogtrop, M.L., Peng, J. & Craig, W.A. In vivo pharmacodynamics of a new oxazolidinone (linezolid). *Antimicrob. Agents Chemother.* **46**, 3484–3489 (2002).

38. Rayner, C.R., Forrest, A., Meagher, A.K., Birmingham, M.C. & Schentag, J.J. Clinical pharmacodynamics of linezolid in seriously ill patients treated in a compassionate use programme. *Clin. Pharmacokinet.* **42**, 1411–1423 (2003).

39. Li, C., Du, X., Kuti, J.L. & Nicolau, D.P. Clinical pharmacodynamics of meropenem in patients with lower respiratory tract infections. *Antimicrob. Agents Chemother.* **51**, 1725–1730 (2007).

40. Moise, P.A., Forrest, A., Bhavnani, S.M., Birmingham, M.C. & Schentag, J.J. Area under the inhibitory curve and a pneumonia scoring system for predicting outcomes of vancomycin therapy for respiratory infections by Staphylococcus aureus. *Am. J. Health Pharm.* **57** Suppl 2, S4–S9 (2000).

41. Moise-Broder, P.A., Forrest, A., Birmingham, M.C. & Schentag, J.J. Pharmacodynamics of vancomycin and other antimicrobials in patients with Staphylococcus aureus lower respiratory tract infections. *Clin. Pharmacokinet.* **43**, 925–942 (2004).

42. Rybak, M.J. The pharmacokinetic and pharmacodynamic properties of vancomycin. *Clin. Infect. Dis.* **42** Suppl 2, S35–S39 (2006).

43. Minichmayr, I.K., Schaeftlein, A., Kuti, J.L., Zeitlinger, M. & Kloft, C. Clinical determinants of target non-attainment of linezolid in plasma and interstitial space fluid: a pooled population pharmacokinetic analysis with focus on critically ill patients. *Clin. Pharmacokinet.* **56**, 617–633 (2017).

44. Tomaselli, F., Maier, A., Matzi, V., Smolle-Jüttner, F.M. & Dittrich, P. Penetration of meropenem into pneumonic human lung tissue as measured by in vivo microdialysis. *Antimicrob. Agents Chemother.* **48**, 2228–2232 (2004).

45. Schaeftlein, A., Minichmayr, I.K. & Kloft, C. Population pharmacokinetics meets microdialysis: benefits, pitfalls and necessities of new analysis approaches for human microdialysis data. *Eur. J. Pharm. Sci.* **57**, 68–73 (2014).

46. Liebchen, U., Kratzer, A., Wicha, S.G., Kees, F., Kloft, C. & Kees, M.G. Unbound fraction of ertapenem in intensive care unit patients. *J. Antimicrob. Chemother.* **69**, 3108–3111 (2014).

47. Kratzer, A., Kees, F. & Dorn, C. Unbound fraction of fluconazole and linezolid in human plasma as determined by ultrafiltration: impact of membrane type. *J. Chromatogr. B Analyt. Technol. Biomed. Life Sci.* **1039**, 74–78 (2016).

Supplementary information accompanies this paper on the *CPT: Pharmacometrics & Systems Pharmacology* website (http://psp-journal.com)